

# PHARMACEUTICAL ENGINEERING®

The Official Magazine of ISPE  
March/April 2024 | Volume 44, Number 2



## Navigating the Asia Pacific Pharmaceutical Landscape for Global Impact

**Evolving China's  
Regulatory System in  
Alignment with ICH**

**Digital Display Labeling  
in Clinical Supplies for  
Clinical Trials**



[ISPE.org/pharmaceutical-engineering](https://ISPE.org/pharmaceutical-engineering)

# ELECTROCHEMICAL TECHNIQUES for Onsite Surface Qualification

By Luis Henrique Guilherme, PhD, Assis Vicente Benedetti, PhD,  
Cecilio Sadao Fugivara, PhD, Peter Hammer, PhD, and Joey Kish, PhD

Pharmaceutical critical utilities are typically built of 316L stainless steel; nevertheless, surface degradation has been reported due to the occurrence of different phenomena. This article aims to explain how field electrochemical techniques using a portable tool can be an effective method for surface inspection, qualification, and monitoring. The surface finish assessment considered different average roughness, obtained by mechanical polishing and electropolishing, and whether the surface was chemically passivated or not, to generate distinct passive films. This was done to prove the sensitivity of the field electrochemical tool using corrosion techniques.

## EXPLANATION OF THE TECHNIQUES USED

The corrosion techniques used included open circuit potential (OCP), cyclic potentiodynamic polarization (CPP), and electrochemical impedance spectroscopy (EIS). X-ray photoelectron spectroscopy (XPS) measurements were performed to characterize the oxide film properties. EIS and XPS demonstrated a close match in terms of oxide thickness determination ( $R^2 > 0.90$ ), and it is worth highlighting the agreement between the chromium to iron (Cr:Fe) ratio and the polarization resistance quantified by XPS and EIS, respectively. In this article, the influences of surface finish techniques on passive film properties and corrosion performance are discussed.

## PHARMACEUTICAL 316L STAINLESS STEEL USAGE

The fine chemical industries, such as pharmaceutical and food-grade aseptic sectors, are used to facing challenges related to the expectations of consumers, price constraints, and strict regulatory requirements. In this scenario, the corrosion and surface contamination of the processing plant equipment plays an important role, as it can compromise product quality and requires adequate selection of the materials, a proper surface finish process, and periodic maintenance [1].

Stainless steel is widely used in pharmaceutical and food-grade industries due to its resistance to corrosion and oxidation, advanced mechanical strength at high temperatures, weldability, and relatively low cost [2–5]. Critical process utilities normally are built using 316L stainless steel due to its excellent passivation properties [6], although it is not immune to corrosion phenomena [7, 8], rouge contamination [9], and biofilm adhesion [10–12] after long-term exposure to industrial processes.

The passivation efficiency of 316L stainless steel depends on its passive film characteristics such as microstructure, surface morphology, oxide layer thickness and uniformity, semiconducting properties, and passivity breakdown in the bioprocess [13–17]. These characteristics change according to the surface finish process; thus, critical utility equipment is designed to achieve a clean and smooth surface that provides high corrosion resistance.

The American Society of Mechanical Engineers: Bioprocessing Equipment (ASME BPE) [18] code specifies the process contact surface finish requirements and acceptance criterion, where the surface finish can be prepared by mechanical polishing or electropolishing. Moreover, a modified passive film by chemical passivation treatment is required according to this code for bioprocess utilities.

The passive film on the surface is a naturally formed 1–3 nanometer (nm) thick layer consisting of chromium-rich oxide/hydroxide phases, whose composition, thickness, and protective action changes dynamically with bioprocessing time [1, 12]. The passive film modified by chemical passivation treatment results in a more resistant surface oxide layer compared to the naturally formed passive film. Indeed, 316L stainless steel passivated surfaces are reported as Cr-rich oxide layers in the form of chromium oxide ( $\text{Cr}_2\text{O}_3$ ), which are mainly responsible for the high passivation ability [14, 19–21].

The main concerns about the use of 316L stainless steel is corrosion damage and the release of metal ions into the processed fluids, which can be hazardous for the end users. Therefore, bioprocess equipment is required to have passivated surfaces instead of natural passive films [1, 18].

However, as there is no field tool and technique available to quantify and qualify the passive film properties, the industrial practices for chemical passivation treatment are not able to assess the efficacy of these treatments. In fact, the ASME BPE code describes electrochemical techniques such as EIS as an advanced

**Table 1:** Finishing methods of American Iron and Steel Institute (AISI) 316L.

Sample ID	Ra <sup>1</sup> ( $\mu\text{m}$ )	Latter Grind- Paper	Electropolished	Passivated
0.8 microns ( $\mu\text{m}$ ) grinding	0.8	220	No	No
0.8 $\mu\text{m}$ passivated	0.8	220	No	Yes
0.3 $\mu\text{m}$ EP	0.3	220	Yes	No
0.3 $\mu\text{m}$ EP passivated	0.3	220	Yes	Yes
0.2 $\mu\text{m}$ grinding	0.2	600	No	No
0.2 $\mu\text{m}$ passivated	0.2	600	No	Yes
0.05 $\mu\text{m}$ EP	0.05	600	Yes	No
0.05 $\mu\text{m}$ EP passivated	0.05	600	Yes	Yes

<sup>1</sup>Ra: roughness average.

tool to measure the passivation property and corrosion resistance of the passivated surface, though the technology is not yet ready for field use [18].

This article aims to elucidate how electrochemical techniques can be applied in field surface finish inspections as an advanced tool for the surface qualification and monitoring of 316L stainless steel tanks and pipelines. It is worth emphasizing that the field electrochemical techniques need to be sensitive enough to differentiate the properties of surface finishes and therefore OCP, CPP, and EIS have been applied. XPS was used to characterize the passive film in terms of oxide chemical composition, thickness, and Cr:Fe ratio.

## METHODS TO QUALIFY INTERNAL SURFACE FINISH

Portable electrochemical minicells have been used to perform surface inspection inside 316L stainless steel tanks to qualify the internal surface finish through the application of electrochemical techniques [22]. The most common surface finish applied to stainless steel tanks was assessed by the portable electrochemical minicell, as shown in Table 1, to prove the tool sensitivity for surface inspection. Each surface finish has an individual Cr:Fe ratio and consequently a specific electrochemical response is expected.

The surface finishing was performed using mechanical polishing, chemical passivation treatment (American Society for Testing and Materials ASTM A380 [23]), electropolishing (EP) according to ASTM B912 [36], and a combination of passivation, as can be seen in Table 1. The XPS and electrochemical measurements were carried out using 1 cm<sup>2</sup> area of a mockup of the finished surface. Additionally, electrochemical tests were employed in practical field inspections of stainless steel tanks. The reproducibility of the electrochemical tests, comparing bench and field measurements, was validated in a previous work [22].

Electrochemical techniques are recognized as the most advanced methods of stainless steel surface characterization [18, 24–26]. Previous studies described the importance of assessing passivated surfaces applying OCP and CPP, Cr-depleted zones, and sensitization (especially for welds) via double-loop electrochemical potentiokinetic reactivation (DL-EPR) [7, 8, 12]. In this article, the field EIS as an onsite technique for passive film properties characterization is introduced.

The portable electrochemical minicell is a portable surface tester capable of quantifying the passive film properties and the corrosion resistance of 316L stainless steel tanks and pipelines. It works as a conventional three-electrodes minicell using a silver chloride electrode (Ag|AgCl|KCl<sup>3</sup> mol/L) as the reference electrode and platinum (Pt) wire as counter electrode that was designed to be used in onsite inspection services [22].

During inspection activities for tanks, the minicell enables multiple measurements in confined spaces to be obtained using a multichannel potentiostat/minicell system. A vacuum cup system was designed to attach the minicell in all positions on the steel surface with a 1.7 millimeter (mm) diameter capillary pair to the tank surface, which was used as the working electrode. Figure 1 shows the portable electrochemical minicell in a field inspection.

Using the portable electrochemical minicell tool in situ, EIS data were recorded in 3.5% mass by volume (m/v) sodium chloride (NaCl) solution at (30±2)°C. The impedance spectra were generated by applying a sinusoidal signal of amplitude 10 millivolt (mV) over the frequency range 0.01 hertz (Hz) to 100 kilohertz (kHz). The resultant spectra were analyzed using the PStrace 5.9 software.

CPP tests were carried out to measure the passivation level and the pitting corrosion resistance in 3.5% (m/v) NaCl solution at (30±2)°C. After stabilization of the open circuit potential (OCP), an anodic polarization scan was performed at a sweep rate of 2.0 mV s<sup>-1</sup>. The anodic scan was reversed after it reached one of the criteria:

Figure 1: A: Portable electrochemical minicell tool for onsite stainless steel surface inspection. B: EIS data acquisition through Bluetooth connection.

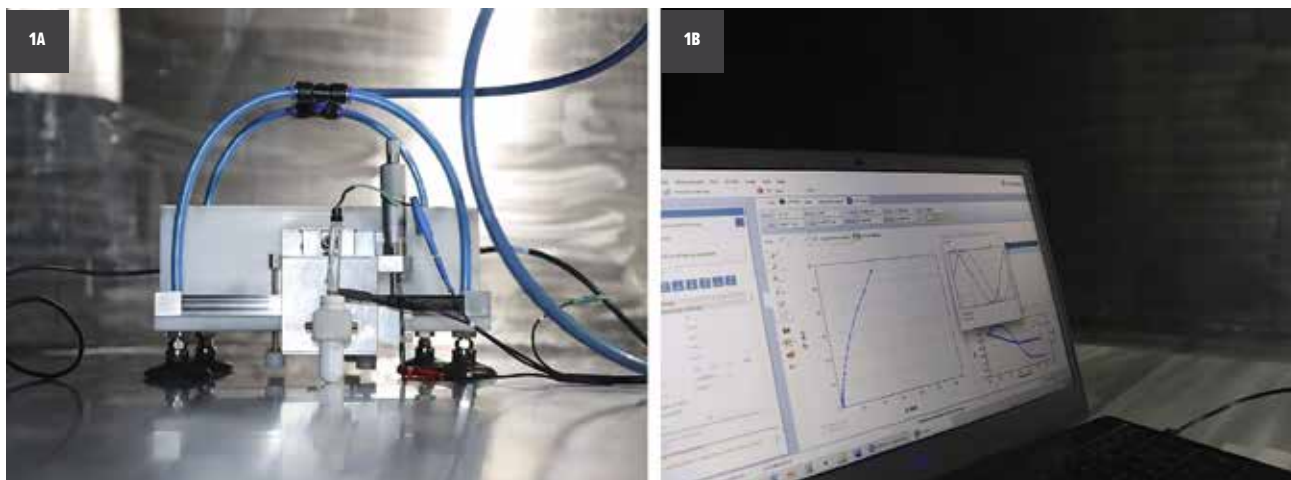


Table 2: Electrochemical techniques and respective acceptance criteria for 316L stainless steel.

Tank Conditions	Objective	Technique	Performance Parameters	Acceptance Criteria
Passivated surface in qualification	Passivation level	EIS	$R_p, Q_{CPE}, \eta^1, C_{eff}$	Passive film thickness ( $\delta$ ): $1 \text{ nm} < \delta < 3 \text{ nm}$
		CPP	$E_{corr}, E_{pit}, E_{prot}$ passivation level	$R_p \geq 2.0 \text{ M}\Omega \text{ cm}^2$ $E_{prot} - E_{corr} > 350 \text{ mV}$
In operation process	Early rouge and corrosion detection	Combining OCP and EIS	$E_{corr}, R_p, Q_{CPE}, \eta^1, C_{eff}$ , EEC (equivalent electrical circuit)	OCP $\geq +10 \text{ mV}$ (Ag AgCl KCl 3 mol/L)
				$R_p \geq 0.5 \text{ M}\Omega \text{ cm}^2$
				$1 \text{ nm} < \delta < 3 \text{ nm}$

<sup>1</sup> Constant phase exponent.

(a) current density of 1 milliamperes per square centimeter ( $\text{mA cm}^{-2}$ ) or (b) potential of 1 volt (V). Then the inspected surfaces were scanned in the cathodic direction to a potential of  $-200 \text{ mV}$  vs. OCP.

Table 2 summarizes the period of evaluation and its respective type of inspection, describing the inspection objective and electrochemical technique for surface inspection. The passivation properties and corrosion resistance of 316L stainless steel were based on literature to specify the acceptance criterion [7, 27].

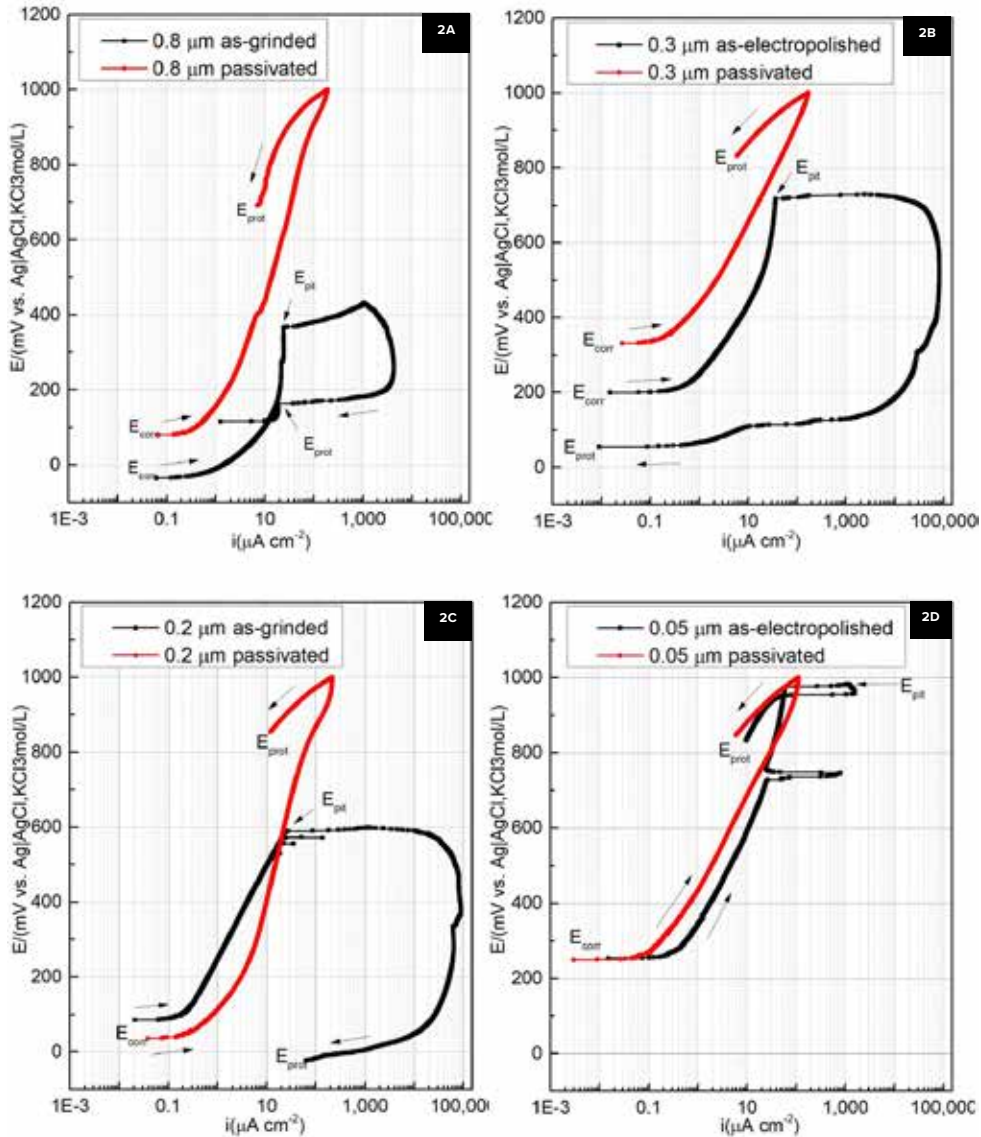
The surface elemental analysis of the samples with different surface treatment was carried out by XPS using a commercial spectrometer (UNI-SPECS UHV) at base pressure lower than  $10^{-7} \text{ Pa}$ .

## RESULTS

Open circuit potential and CPP curves in 3.5% (m/v) NaCl solution at  $(30 \pm 2)^\circ\text{C}$  were performed after reaching a stable OCP for all surface finishes and the performance parameters are presented in Figure 2. In Figure 2, each figure shows the CPP curves of the surfaces in the conditions as polished and passivated. All polarization curves showed a passive behavior during the anodic scan. The surface performance was quantified based on the CPP parameters shown in Table 3: corrosion potential ( $E_{corr}$ ), pitting corrosion ( $E_{pit}$ ), corrosion protection ( $E_{prot}$ ), and passivation current density ( $i_{pass}$ ).

It is worth analyzing what sort of hysteresis was observed during the positive or negative potential reversal. The hysteresis

**Figure 2:** Cyclic potentiodynamic polarization curves obtained for 316L stainless steel in 3.5% (m/v) NaCl, at  $(30 \pm 2)^\circ\text{C}$ , and  $2.0 \text{ mV s}^{-1}$  of A:  $0.8 \mu\text{m}$  as-grinded and passivated surface; B:  $0.3 \mu\text{m}$  as-electropolished and passivated surface; C:  $0.2 \mu\text{m}$  as-grinded and passivated surface; and D:  $0.05 \mu\text{m}$  as-electropolished and passivated surface.



behavior shows either pitting growth or surface repassivation, findings which have been discussed in a previous paper [7]. Based on the electrochemical parameters, it is safe to state that the mechanical polished surfaces generated inferior passivation properties, whereas the electropolished surface significantly decreases the passivation current density and increases the pitting resistance. Nevertheless, mechanical and electropolished surfaces have registered the pitting corrosion in a potential range of 300–600 mV and 600–900 mV, respectively. Furthermore, a positive hysteresis was observed after reversing the potential scan, indicating that the pitting continues to grow. In contrast, the

passivated surfaces presented a higher corrosion resistance evidenced by the absence of pitting potential, reduced passivation current density, and negative hysteresis.

The passivation level (PL) represents the anodic passivation range of the material (equation 1) based on the electrochemical parameters derived from the CPP curves: corrosion potential ( $E_{\text{corr}}$ ) and corrosion protection potential ( $E_{\text{prot}}$ ). If  $E_{\text{prot}}$  is nobler than  $E_{\text{corr}}$ , there is a potential range where the passive film is stable and localized corrosion such as pitting, crevice, or cracking will not develop or grow [24]. The acceptance criterion for the PL, according to equation 1, is 350 mV<sup>7</sup>. The corrosion resistance parameters

**Table 3:** PL assessment of studied surfaces obtained in 3.5% NaCl solution.

Surface Finish	$i_{pass @ 0.3V}$ ( $\mu A cm^{-2}$ )	$E_{corr}$ (mV)	$E_{prot}$ (mV)	$E_{pit}^1$ (mV)	PL (mV)
0.8 $\mu m$ grinded	24.5	-35	+162	+365	+197
0.8 $\mu m$ passivated	3.7	+90	+692	+1,000	+602
0.3 $\mu m$ EP	2.1	+200	+54	+716	-146
0.3 $\mu m$ EP passivated	0.02	+331	+831	+1,000	+500
0.2 $\mu m$ grinded	1.6	+85	-23	+588	-108
0.2 $\mu m$ passivated	6.3	+40	+854	+1,000	+814
0.05 $\mu m$ EP	0.6	+253	+832	+975	+579
0.05 $\mu m$ EP passivated	0.2	+250	+850	+1,000	+600

$E_{pit} = 1,000$  mV indicates that stable pit nucleation and growth did not occur.

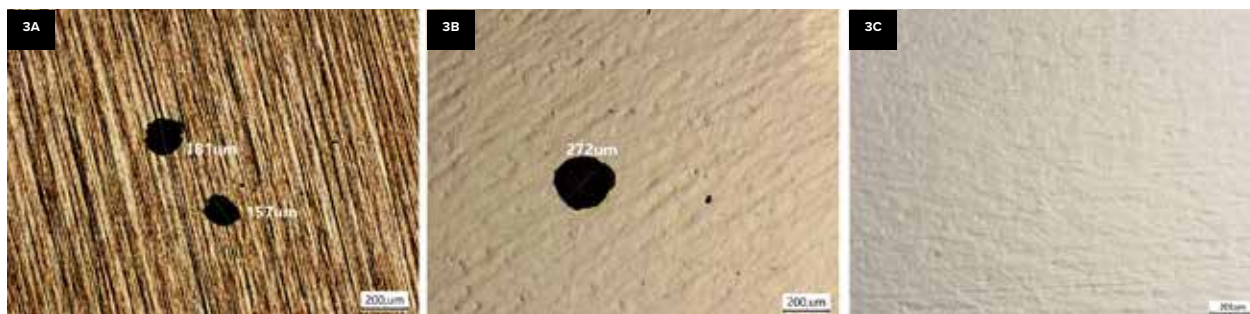
obtained from the OCP and CPP curves in 3.5% NaCl were performed after 12 months of reactor operation and are summarized in Table 3.

$$PL = E_{prot} - E_{corr} \quad (1)$$

Figure 3 shows optical micrographs for 316L stainless steel scanned surface area after CPP testing. It shows stable pits for grinded and electropolished surfaces (see Figure 3A and 3B), whereas the passivated surfaces remained pitting-free (see Figure 3C).

EIS spectra in the Nyquist representation recorded during immersion in the 3.5% (m/v) NaCl at (30±2)°C are reported in Figure 4. They are portions of depressed semicircles, that can be fitted with the simple EEC model for a compact film [1], as can be seen in Figure 4, where  $R_{el}$  is the electrolyte resistance,  $R_p$  is the polarization resistance and CPE is a constant phase element introduced to account for the heterogeneity of oxide layer which cannot be represented by a pure capacitance.

**Figure 3:** Optical micrographs of 316L stainless steel scanned surface area after CPP measurements of A: Ra = 0.8  $\mu m$  grinded surface with  $E_{pit} = +365$  mV; B: Ra = 0.3  $\mu m$  electropolished surface with  $E_{pit} = +716$  mV; and C: Ra = 0.3  $\mu m$  electropolished and passivated surface without  $E_{pit}$ . Electrolyte: 3.5% (m/v) NaCl.



EIS spectra were fitted using an  $R(R_{CPE})$  EEC. The passive film thickness was estimated according to the power law model [28] to be in the range of 1–3 nm, in agreement with previously reported values [1, 21]. The fitting parameters, reported in Table 4, suggest that RP was substantially increased in the case of passivation treatment for all surface finishes (mechanical and electropolished).

Furthermore, the best-fit exponent ( $n$ ) of the constant phase element yields values < 1, as expected for passive films on stainless steel [1, 29]. As seen in equation 2, this behavior is explained by the formation of a passive film with a resistivity gradient going from the metal–oxide interface to the oxide–electrolyte interface, where  $Q$  vs.  $n$  can be described according to the power law model [30]:

$$Q = \frac{(\epsilon\epsilon_0)^n}{g\delta\rho_\delta^{1-n}} \quad (2)$$

where  $\epsilon$  is the passive film dielectric constant,  $\epsilon_0$  is the vacuum permittivity ( $8.8542 \times 10^{-14}$  F cm<sup>-1</sup>),  $\delta$  is the oxide layer thickness,  $\rho_\delta$  is the resistivity of the oxide at the oxide–solution interface, and  $g$  is a numerical function given by [29]:

$$g = 1 + 2.88(1 - n)^{2.375} \quad (3)$$

Considering that the CPE results from a dielectric response of the material, it allows us to determine the film thickness,  $d$ , in terms of an effective capacitance and dielectric constant,  $\epsilon$ , according to [28]:

$$\delta = \frac{\epsilon\epsilon_0}{C_{eff}} \quad (4)$$

Combining equations 2 and 4 yields an expression for the effective capacitance as [30, 31]:

$$C_{eff} = gQ(\rho_\delta\epsilon\epsilon_0)^{1-n} \quad (5)$$

The passive film thickness estimated assuming a dielectric constant of chromium and iron oxide of 12 and  $\rho_\delta = 500 \Omega cm$  [1] is shown in Table 4.

The mechanical polished surface demonstrated a passive film thickness between 2.1–2.3 nm, whereas the values of the electropolished surface were thinner in the range of 1.5–2.1 nm. As a rule, all passivated surfaces were reported to have the thinnest passive film of about 0.9–1.4 nm, showing the highest passivation properties and corrosion resistance [19]. This is explained by the fact that the naturally formed passive film has a nonuniform Cr-rich layer and a thicker Fe-rich oxide and hydroxide, whereas the passive film modified by passivation treatment is composed of a thin, uniform, and compact Cr-rich oxide layer [6, 13, 14].

The obtained passive film thickness values were confirmed by XPS analysis resulting from the exponential attenuation of the metallic Fe  $2p_{3/2}$  peak intensity. A comparison of the layer thicknesses in Table 4 obtained by both techniques shows a close match between the values, using two independent methods. To investigate the elemental composition and identify the phases that form the passive layer a quantitative analysis of the deconvoluted XPS spectra was performed. Table 5 displays the atomic percentages of the metallic elements for different treatment conditions, including the as-received alloy as reference and highlighting the Cr to Fe ratio.

## DISCUSSION

Surface qualification of 316L stainless steel tanks using field electrochemical measurements via portable electrochemical minicell was applied as a promising tool to ensure high product quality. The bioprocessing tanks are required to be submitted to a surface qualification process before introducing them to the industrial process, and ASME BPE code describes the electrochemical techniques as an advanced inspection method, although this technology is not yet ready for field inspections. As a complementary technique, XPS measurements are allowed to characterize the passive film, supporting the efficacy of portable electrochemical minicells for field surface inspection.

Comparing the corrosion resistance performance of the different treatments, it is safe to state that the passivated surface reached the highest parameters for all conditions, highlighting an approved PL quite superior of the acceptance criterion of 350 mV. In addition, it is worth pointing out that the absence of pitting corrosion and the negative hysteresis running in a quite reduced passivation current density confirms that the passive film is composed by Cr-rich and uniform oxide [14, 15, 20, 24, 32–35]. On the other hand, an ASTM B912 [36]

**Figure 4:** EIS spectra in Nyquist representation recorded during immersion in 3.5% (m/v) NaCl for 316L stainless steel passive film with surface finish: A: 0.8  $\mu\text{m}$  grinded and 0.8  $\mu\text{m}$  grinded and passivated; B: 0.3  $\mu\text{m}$  electropolished and 0.3  $\mu\text{m}$  electropolished and passivated; C: 0.2  $\mu\text{m}$  grinded and 0.2  $\mu\text{m}$  grinded and passivated; and D: 0.05  $\mu\text{m}$  electropolished and 0.05  $\mu\text{m}$  electropolished and passivated.

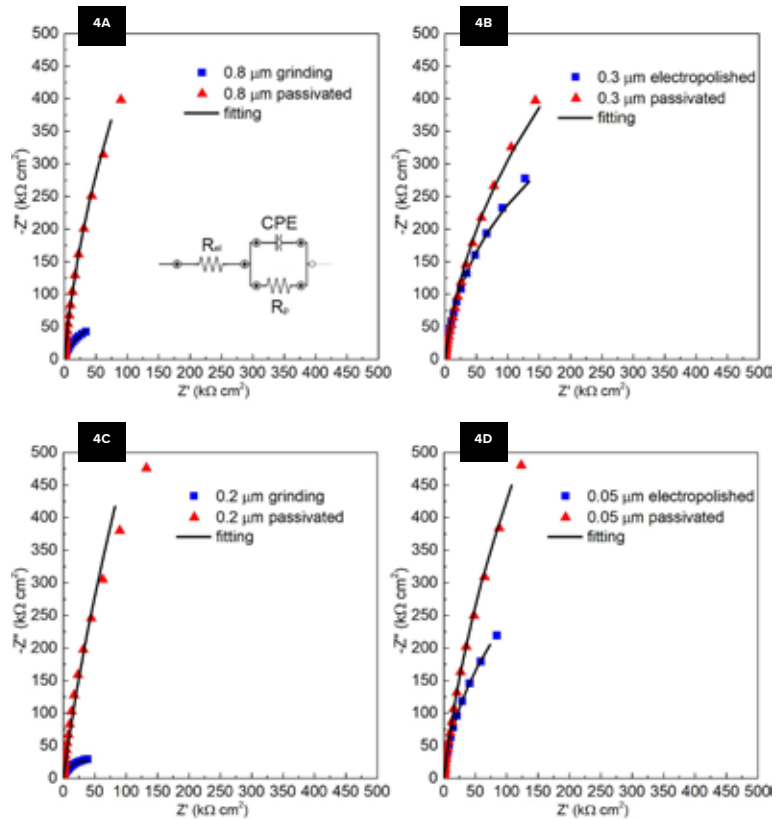


**Table 4:** XPS and EIS surface characterization.

Sample	$R_{el}$ (W) $\text{cm}^2$	$R_p$ (M $\Omega$ ) $\text{cm}^2$	CPE $Y_0$ (mF $\text{cm}^2$ )	$n$	$\chi^2/10^{-3}$	$d_{EIS}$ (nm)	$d_{XPS}$ (nm)
0.8 $\mu\text{m}$ grinding	5.4	0.15	239	0.81	1.8	2.33	2.37
0.8 $\mu\text{m}$ passivated	5.1	3.52	46	0.91	1.6	1.55	1.74
0.3 $\mu\text{m}$ EP	5.1	0.86	50	0.91	1.6	1.44	1.50
0.3 $\mu\text{m}$ EP passivated	5.4	1.72	54	0.92	0.8	1.12	1.02
0.2 $\mu\text{m}$ grinding	4.7	0.07	208	0.82	2.7	2.14	2.80
0.2 $\mu\text{m}$ passivated	4.3	8.14	54	0.91	4.5	1.36	1.31
0.05 $\mu\text{m}$ EP	3.7	0.57	118	0.85	2.3	2.14	2.30
0.05 $\mu\text{m}$ EP passivated	4.4	3.96	51	0.92	1.1	1.09	0.92

**Table 5:** Atomic composition of 316L stainless steel surfaces obtained by XPS.

Sample	Cr (at.%)	Fe (at.%)	Ni (at.%)	Molybdenum (Mo) (at.%)	Manganese (Mn) (at.%)	Cr:Fe Ratio
As received	23.9	65.2	5.7	3.0	2.2	0.4
0.8 μm grinding	29.7	62.1	2.1	5.1	1.0	0.6
0.8 μm passivated	52.6	34.9	5.6	5.6	1.3	1.5
0.3 μm EP	51.2	31.4	4.7	11.6	1.2	1.6
0.3 μm EP passivated	55.1	27.5	10.7	5.6	1.1	2.0
0.2 μm grinding	35.1	59.7	1.2	3.8	1.2	0.6
0.2 μm passivated	61.9	25.2	4.8	7.1	1.0	2.5
0.05 μm EP	34.0	50.6	6.8	7.8	0.8	0.7
0.05 μm EP passivated	57.4	28.5	7.2	5.1	1.8	2.1

**Figure 5:** Correlation between the XPS and EIS passive film thickness data.

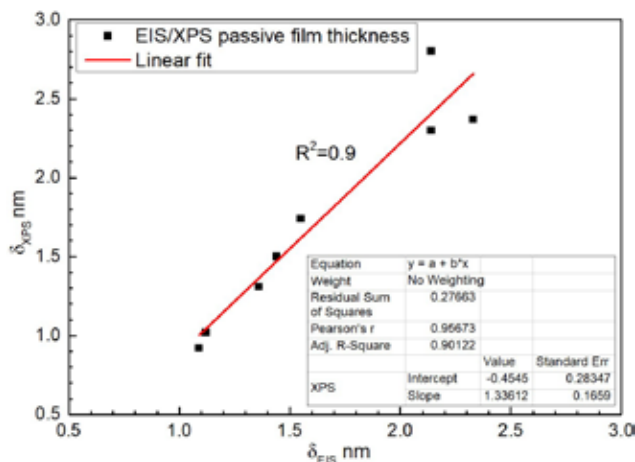
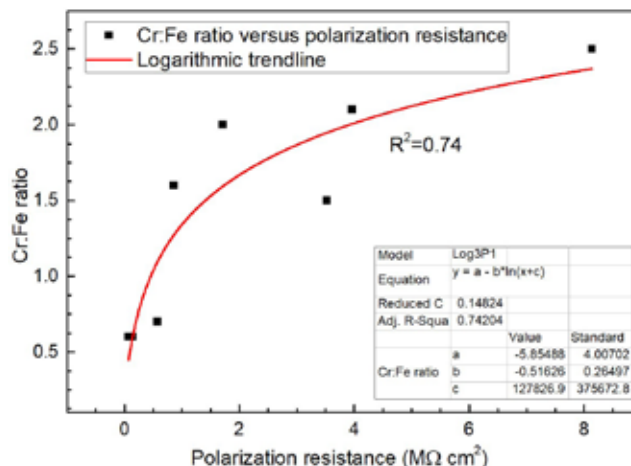


**Figure 6:** Parabolic relation between Cr:Fe ratio and polarization resistance.



electropolished surface did not perform as resistant as expected considering that ASME BPE specify that the electropolished surfaces are considered as passivated.

However, the maximum corrosion resistance was obtained when combining the electropolishing process with the chemical passivation treatment in sequence. The grinded surface finish is a concern due to the poor pitting potential, a nonacceptable PL, and a high passivation current density. On the other hand, electropolished surface and grinded surface finishes were improved in terms of corrosion resistance by the chemical passivation, achieving acceptable PL after the treatment.

XPS measurements demonstrated that the passive films on 316L austenitic stainless steel had a structure as previously

described, which consists of an inner region composed of a Cr-rich oxide layer ( $Cr_2O_3$ ) in contact with the metallic substrate, whereas the outermost layer is composed of  $Cr(OH)_3$  and Fe-rich oxides and hydroxides: iron(II) oxide ( $FeO$ ), iron(III) oxide ( $Fe_2O_3$ ), iron(III) oxide-hydroxide ( $FeOOH$ ).

Besides these iron species, magnetite ( $Fe_3O_4$ ) and  $Fe(OH)_2$  were also reported to compose this layer [14, 15, 38–41]. However, a closer look at the data obtained for different surface treatments revealed distinct features. On mechanical polished surfaces grew a natural passive film, with a thick oxide layer in a range of 2.4–2.8 nm, chemically characterized as Fe-rich oxides with a low Cr:Fe ratio of about 0.6 (see Tables 4 and 5).

When compared to the mechanical polished surfaces, the



**Table 6: Conclusion matrix.**

Criteria	Conclusion
Passive film thickness	A linear relation between the passive film thickness obtained by EIS and XPS measurements was found. The passive film thickness determined by EIS and XPS techniques were very close, with residual values varying within an interval of 0.2 nm. This means that it is safe to state that onsite electrochemical tests provide consistent data in terms of passive film properties.
Correlation of Cr:Fe ratio and Rp	The polarization resistance and the Cr:Fe ratio show parabolic power law dependence, allowing us to relate EIS field inspection results with those of XPS for the qualification of the passivation treatment procedure. This is important information for onsite measurements that allows for the estimation of the tank resting time after passivation treatment.
Sensitivity of the tool	The portable electrochemical minicell was able to differentiate the surface resistance of different surface finishes, where the distinguished value of Cr:Fe ratio was known. The most common surface finishes for pharmaceutical tanks were assessed and the portable electrochemical minicell was able to differentiate the surface resistance. Each surface finish had a specific Cr:Fe ratio, and it was measured distinguished polarization resistance, which proved the sensitivity of the tool.
Bottom line	Field electrochemical measurements applying EIS technique has proven to be accurate in determining passive film properties, and it can be a powerful tool for qualification and monitoring of the passivation properties of stainless steel surfaces.

electropolished surfaces grew a thinner (1.5–2.3 nm) and more Cr-rich passive film, resulting in a Cr:Fe ratio of 1.6–2.3 nm. The latter value highlights the 0.3 $\mu$ m-EP sample. Even though electropolished surfaces provided an improved passive oxide when compared to the mechanical polished surfaces, it is important to note that in both cases an Fe-rich and nonuniform passive film was formed on the surface, as indicated by the breakdown potential in cyclic polarization tests.


The main hypothesis taken into consideration is the fact that the mechanical and electropolishing processes promoted the growth of the Fe-rich layer [18, 20]. On the other hand, the passive film modified by chemical passivation treatment provided the highest passivation properties with the Cr:Fe ratio of up to 2.5 nm (see Table 5) due to the selective dissolution of iron. The layer consists mainly of Cr<sub>2</sub>O<sub>3</sub> and Cr(OH)<sub>3</sub> phases, which are responsible for the high corrosion resistance [41] (see Table 4). These surfaces showed the thinnest passive film being in the range of 1.0–1.7 nm, containing a reduced quantity of Fe oxides, a small fraction of Mo oxides, and traces of nickel and Mn oxides.

Portable electrochemical minicell is a portable tool used to measure the passivation properties and corrosion resistance of stainless steel tank surfaces in field conditions. This work demonstrates that, using portable electrochemical inspection techniques, an accurate onsite tank surface performance can be determined in terms of corrosion resistance and passivation parameters.

The results are consistent with those obtained by XPS, confirming the passive film thickness values obtained by EIS, and associating the high corrosion resistance, obtained from the OCP and CPP curves, to the distinct structure of the thin passive layer. These notable results are shown in Figures 5 and 6. Figure 5 displays a linear trendline correlating the passive film thickness determined by both techniques with R-squared values > 0.90, which represents a good fit to the data.

Additionally, as can be seen in Figure 6, a parabolic relation between polarization resistance and Cr:Fe ratio was found in a preliminary assessment. This demonstrated the great potential of the portable electrochemical minicell technique for field surface qualification. However, further studies are needed to establish this method as the standard test for stainless steel tanks.

## CONCLUSION

The portable electrochemical minicell's efficacy was tested through the inspection of different surface finishes of 316L stainless steel typically applied in tanks and facilities. Table 6 shows the conclusions according to the performance perspective of the portable tool. Field electrochemical measurements applying EIS technique has proven to be accurate in determining passive film properties, and it can be a powerful tool for qualification and monitoring of the passivation properties of stainless steel surfaces. 

## Acknowledgments

The authors would like to thank the São Paulo Research Foundation (FAPESP) for providing financial support for this research (Proc. no. 2021/11684-4).

## References

- Santamaria, M., G. Tranchida, and F. Di Franco. "Corrosion Resistance of Passive Films on Different Stainless Steel Grades in Food and Beverage Industry." *Corrosion Science*, 173 (2020). doi:10.1016/j.corsci.2020.108778
- Lippold, J. C. *Welding Metallurgy and Weldability*. Hoboken, NJ: Wiley, 2015.
- Reccagni, P., L. H. Guilherme, Q. Lu, M. F. Gittos, and D. L. Engelberg. "Reduction of Austenite-Ferrite Galvanic Activity in the Heat-Affected Zone of a Gleeble-Simulated Grade 2205 Duplex Stainless Steel Weld." *Corrosion Science*, 161 (2019). doi:10.1016/j.corsci.2019.108198

4. Guilherme, L. H., P. Reccagni, A. V. Benedetti, C. S. Fugivara, and D. L. Engelberg. "Corrosion Assessment of ASME Qualified Welding Procedures for Grade 2101 Lean Duplex Stainless Steel." *Corrosion* 75, no. 10 (2019): 1216–29. doi:10.1016/j.corsci.2019.108198
5. Guilherme, L. H., A. V. Benedetti, C. S. Fugivara, R. Magnabosco, and M.F. Oliveira. "Effect of MAG Welding Transfer Mode on Sigma Phase Precipitation and Corrosion Performance of 316L Stainless Steel Multi-pass Welds." *Journal of Materials Research and Technology* 9, no. 5 (2020): 10537–49. doi:10.1016/j.jmrt.2020.07.039
6. Montemor, M. F., M. G. S. Ferreira, N. E. Hakiki, and M. Da Cunha Belo. "Chemical Composition and Electronic Structure of the Oxide Films Formed on 316L Stainless Steel and Nickel Based Alloys in High Temperature Aqueous Environments." *Corrosion Science* 42, no. 9 (2000): 1635–50. doi:10.1016/S0010-938X(00)00012-3
7. Guilherme, L. H., C. S. Fugivara, and A. V. Benedetti, "On-Site Weld Quality Assessment and Qualification for Stainless Steels Tanks." *Eclética Química Journal* 47, no. 3 (2022): 55–65. doi:10.26850/1678-4618eqj.v47.3.2022.p55-65
8. Guilherme, L. H., A. V. Benedetti, C. S. Fugivara, and D. Engelberg. "Passivation Level of AISI 316L Aseptic Tank Surface Quantified by On-Site Electrochemical Techniques." *Materials Research* 25 (2022): 1–6. doi:10.1590/1980-5373-MR-2021-0623
9. Di Franco, F., M. Santamaria, G. Massaro, and F. Di Quarto, "Photoelectrochemical Monitoring of Rouging and De-Rouging on AISI 316L." *Corrosion Science* 116 (2017): 74–87. doi:10.1016/j.corsci.2016.12.016
10. Tran, T. T. T., K. Kannoorpatti, A. Padovan, and S. Thennadil. "A Study of Bacteria Adhesion and Microbial Corrosion on Different Stainless Steels in Environment Containing *Desulfovibrio Vulgaris*." *Royal Society Open Science* 8 (2021): 201577. doi:10.1098/rsos.201577
11. Di Franco, F., G. Tranchida, D. Pupillo, G. Ghersi, P. Cinà, S. Virtanen, and M. Santamaria, "Effect of *E. coli* Biofilm Formation and Removal on Passive Films on AISI 316L During Fermentation Processes." *Corrosion Science* 185 (2021): 109430. doi:10.1016/j.corsci.2021.109430
12. Guilherme, L. H., C. S. Fugivara, and A. V. Benedetti. "Surface Qualification of AISI 316L Bioprocessing Tanks Applying On-site Electrochemical Measurements." *Matéria (Rio Janeiro)* 27, no. 4 (2022): 1–14. doi:10.1590/1517-7076-RMAT-2022-0183
13. Shih, C.-C., C.-M. Shih, Y.-Y. Su, L. H. J. Su, M.-S. Chang, and S.-J. Lin. "Effect of Surface Oxide Properties on Corrosion Resistance of 316L Stainless Steel for Biomedical Applications." *Corrosion Science* 46 (2004): 427–41. doi:10.1016/S0010-938X(03)00148-3
14. Wallinder, D., J. Pan, C. Leygraf, and A. Delblanc-Bauer. "Eis and XPS Study of Surface Modification of 316LVM Stainless Steel After Passivation." *Corrosion Science* 41 (1998): 275–89. doi:10.1016/S0010-938X(98)00122-X
15. Xu, H., L. Wang, D. Sun, and H. Yu. "The Passive Oxide Films Growth on 316L Stainless Steel in Borate Buffer Solution Measured by Real-Time Spectroscopic Ellipsometry." *Applied Surface Science* 351 (2015): 367–73. doi:10.1016/j.apsusc.2015.05.165
16. Olsson, C.-O. A., and D. Landolt. "Film Growth During Anodic Polarization in the Passive Region on 304 Stainless Steels with Cr, Mo, or W Additions Studied with EQCM and XPS." *Journal of The Electrochemical Society* 148 (2001): B438. doi:10.1149/1.1404969
17. Lorang, G., M. Da Cunha Belo, A. M. P. Simões, and M. G. S. Ferreira. "Chemical Composition of Passive Films on AISI 304 Stainless Steel." *Journal of The Electrochemical Society* 141 (1994): 3347–56. doi:10.1149/1.2059338
18. American Society of Mechanical Engineers. *Bioprocessing Equipment, BPE - 2022*. New York, NY: ASME, 2022.
19. Zakerin, N., and K. Morshed-Behbahani. "Electrochemical Insight into the Role of H<sub>2</sub>O<sub>2</sub> in Galvanostatic Passivation of AISI 316L Austenitic Stainless Steel in Citric Acid Electrolyte." *Metallurgical and Materials Transactions A* 52 (2021): 3247–56. https://link.springer.com/10.1007/s11661-021-06283-9
20. Shahryari, A., S. Omanovic, and J. A. Szpunar. "Electrochemical Formation of Highly Pitting Resistant Passive Films on a Biomedical Grade 316LVM Stainless Steel Surface." *Material Science and Engineering: C* 28, no. 1 (2008): 94–106. doi:10.1016/j.msec.2007.09.00
21. Olsson, C.-O. A., and D. Landolt. "Passive Films on Stainless Steels—Chemistry, Structure and Growth." *Electrochimica Acta* 48, no. 9 (2003): 1093–104. doi:10.1016/S0013-4686(02)00841-1
22. Guilherme, L. H., A. V. Benedetti, and C. S. Fugivara. "A Portable Electrochemical Microcell for Weld Inspection of Duplex Stainless Steel Tanks." *Corrosion* 75, no. 4 (2019): 340–8. doi:10.5006/3004
23. ASTM International. *ASTM A380/A380M-17: Standard Practice for Cleaning, Descaling, and Passivation of Stainless Steel Parts, Equipment, and Systems*. West Conshohocken, PA: ASTM International, 2013.
24. Esmailzadeh, S., M. Aliofkhaeaei, and H. Sarlak. "Interpretation of Cyclic Potentiodynamic Polarization Test Results for Study of Corrosion Behavior of Metals: A Review." *Protection of Metals and Physical Chemistry of Surfaces* 54 (2018): 976–89. http://link.springer.com/10.1134/S207020511805026X
25. ASTM International. *ATSM A262-1: Standard Practices for Detecting Susceptibility to Intergranular Attack in Austenitic Stainless Steels*. West Conshohocken, PA: ASTM International, 2021.
26. Boissy, C., C. Alemany-Dumont, and B. Normand. "EIS Evaluation of Steady-State Characteristic of 316L Stainless Steel Passive Film Grown in Acidic Solution." *Electrochemistry Communications* 26 (2013): 10–2. doi:10.1016/j.elecom.2012.09.040
27. Deng, B., Y. Jiang, J. Xu, T. Sun, J. Gao, L. Zhang, et al. "Application of the Modified Electrochemical Potentiodynamic Reactivation Method to Detect Susceptibility to Intergranular Corrosion of a Newly Developed Lean Duplex Stainless Steel LDX2101." *Applied Surface Science* 52 (2010): 969–77. doi:10.1016/j.corsci.2009.11.020
28. Benoit, M., C. Bataillon, B. Gwinner, F. Miserque, M. E. Orazem, C. M. Sánchez-Sánchez, et al. "Comparison of Different Methods for Measuring the Passive Film Thickness on Metals." *Electrochimica Acta* 201 (2016): 340–7. doi:10.1016/j.electacta.2015.12.173
29. Hirschorn, B., M. E. Orazem, B. Tribollet, V. Vivier, I. Frateur, and M. Musiani. "Constant-Phase-Element Behavior Caused by Resistivity Distributions in Films: I. Theory." *Journal of Electrochemical Society* 157, no. 12 (2010): C452. doi:10.1149/1.3499564
30. Orazem, M. E., B. Tribollet, V. Vivier, D. P. Riemer, E. White, and A. Bunge. "On the Use of the Power-Law Model for Interpreting Constant-Phase-Element Parameters." *Journal of the Brazilian Chemical Society* 25 (2014): 532–9. doi:10.5935/0103-5053.20140021
31. Hirschorn, B., M. E. Orazem, B. Tribollet, V. Vivier, I. Frateur, and M. Musiani. "Determination of Effective Capacitance and Film Thickness from Constant-phase-element Parameters." *Electrochimica Acta* 55 (2010): 6218–27. doi:10.1016/j.electacta.2009.10.065
32. Xiong, J., S. Agarwala, M. Y. Tan, and M. Forsyth. "The Restoration of the Passivity of Stainless Steel Weldments in Pickling Solutions Observed Using Electrochemical and Surface Analytical Methods." *Corrosion* 71 (2015): 1248–56.
33. Choi, Kang Hoon. "Electrochemical Passivation of 316L Stainless Steel for Biomedical Applications: A Method for Improving Pitting Corrosion Resistance Via Cyclic Potentiodynamic Polarization." Dissertation, McGill University Libraries, 2019.
34. Samim, P. M., and A. Fattah-alhosseini. "Enhancing the Electrochemical Behavior of AISI 304 Stainless Steel by Cyclic Potentiodynamic Passivation (CPP) Method." *Analytical and Bioanalytical Electrochemistry* 8 (2016): 717–731.
35. Saadi, S. A., Y. Yi, P. Cho, C. Jang, and P. Beeley. "Passivity Breakdown of 316L Stainless Steel During Potentiodynamic Polarization in NaCl Solution." *Corrosion Science* 111 (2016): 720–7. doi:10.1016/j.corsci.2016.06.011
36. ASTM International. *ATSM B912-02: Standard Specification for Passivation of Stainless Steels Using Electropolishing 1*. West Conshohocken, PA: ASTM International, 2018.
37. Carmezim, M. J., A. M. Simões, M. F. Montemor, and M. Da Cunha Belo. "Capacitance Behaviour of Passive Films on Ferritic and Austenitic Stainless Steel." *Corrosion Science* 47, no. 3 (2005): 581591. doi:10.1016/j.corsci.2004.07.002
38. Fattah-alhosseini, A., A. Saatchi, M. A. Golozar, and K. Raeissi. "The Passivity of AISI 316L Stainless Steel in 0.05 M H<sub>2</sub>SO<sub>4</sub>." *Journal of Applied Electrochemistry* 40 (2010): 457–61. http://link.springer.com/10.1007/s10800-009-0016-y

39. Nie, J., L. Wei, Y. Jiang, Q. Li, and H. Luo. "Corrosion Mechanism of Additively Manufactured 316 L Stainless Steel in 3.5 Wt.% NaCl Solution." *Materials Today Communications* 26 (2021): 101648. doi:10.1016/j.mtcomm.2020.101648
40. Shintani, D., T. Ishida, H. Izumi, T. Fukutsuka, Y. Matsuo, and Y. Sugie. "XPS Studies on Passive Film Formed on Stainless Steel in a High-Temperature and High-Pressure Methanol Solution Containing Chloride Ions." *Corrosion Science* 50 (2008): 2840–5. doi:10.1016/j.corsci.2008.07.006
41. Hong, T., T. Ogushi, and M. Nagumo. "The Effect of Chromium Enrichment in the Film Formed by Surface Treatments on the Corrosion Resistance of Type 430 Stainless Steel." *Corrosion Science* 38, no. 6 (1996): 881–8. doi:10.1016/0010-938X(96)00174-6

### About the authors

**Luis Henrique Guilherme, PhD**, is Technical Director of Group ACW. He provides engineering services for inspections, electropolishing, and passivation treatments in projects based in Brazil, the US, Canada, the UK, and Germany. He is the Principal Researcher at PIPE/FAPESP for industrial applied research of field electrochemical surface inspections and optimization of passivation treatments of stainless steel. He is the author of more than 10 peer-reviewed articles and two granted patents. He has experience with welding process and metallurgy, design of pressure vessels and tanks, EIS, chemical surface analysis, passive film characterization and modification, surface engineering, and duplex stainless steel. He holds a PhD in materials science and engineering focused on surface engineering and welding of stainless steel for bioprocessing applications. He joined ISPE in 2023.

**Cecilio Sadao Fugivara, PhD**, is an Assistant Professor in electrochemistry and experimental physical chemistry. His research is in localized corrosion, corrosion monitoring by electrochemical methods, and corrosion protection of steel by volatile corrosion inhibitors.

**Peter Hammer, PhD**, is a Researcher/Professor at São Paulo State University, a member of the Physical Chemistry Materials Group, and Head of the Photoelectron Spectroscopy Laboratory of the Institute of Chemistry. He specializes in physical chemistry of materials and condensed matter physics, with an emphasis on the development and structural characterization of advanced nanostructured materials using various spectroscopic techniques with a focus on photoelectron spectroscopy (XPS/UPS). His research fields include the development of multifunctional organic–inorganic hybrid materials with application in anticorrosive biocompatible coatings, carbon nanostructures, and carbon–ceramic nanocomposites applied in the heterogeneous catalysis.

**Joey Kish, PhD**, is Scientific Director of the McMaster's Centre for Automotive Materials and Corrosion. He also leads a research team focused on corrosion and its control of structural engineering alloys in terms of determining influence of metallurgical aspects on the controlling anode and cathode processes across multi-length scales from macro (weld zones) down to nano (grain boundary and second phase particles). He joined McMaster in 2008 after spending 10 years working in the industry: two years as a Materials Specialist with NORAM Engineering and Constructors Ltd. and eight years as a Corrosion Scientist at the Pulp and Paper Research Institute of Canada.

**Assis Vicente Benedetti, PhD**, is a Professor of undergraduate, graduate, and postgraduate courses in physical chemistry at São Paulo State University, Institute of Chemistry. He is also Senior Professor at the Institute of Chemistry, Editor-in-Chief of *Eclética Química*, and an expert in electrochemistry, corrosion, micro electrochemistry, thermal spray, polymeric and organic–inorganic hybrid coatings, corrosion protection, electrodeposition, and electrochemical of minerals. He has experience with modified electrodes, thermal spray techniques, microscopic techniques, EIS, and chemical surface analysis. He holds a bachelor's degree in chemistry and pharmacy, a master's degree in physical chemistry, and a PhD in physical chemistry and was a postdoctorate student at the University of Barcelona, Barcelona, Spain.

## UPCOMING ISPE CONFERENCES



**2024 ISPE Aseptic Conference**  
12-13 March 2024  
Vienna, Austria and Virtual



**2024 ISPE Annual Meeting & Expo and Annual ISPE Foundation Golf Tournament**  
13-16 October 2024  
Orlando, FL, USA and Virtual



**2024 ISPE Europe Annual Conference**  
16-18 April 2024  
Lisbon, Portugal and Virtual



**2024 ISPE Pharma 4.0™ & Annex 1 Conference**  
10-11 December 2024  
Rome, Italy and Virtual



**2024 ISPE Biotechnology Conference**  
17-18 June 2024  
Boston, MA, USA and Virtual



**2025 ISPE Facilities of the Future Conference**  
27-28 January 2025  
San Francisco, CA, USA and Virtual

REGISTER AT [ISPE.org/Conferences](https://www.ispe.org/conferences)

